Surface measurements of energy and CO_2 fluxes within an Iowan wind farm: assessing wind power impacts on intensively managed agricultural croplands

Daniel A. Rajewski[1], Russell K. Doorenbos[2], and Kristopher K. Spoth[2]

[1]Department of Geological and Atmospheric Sciences, [2]Department of Agronomy, Iowa State University, Ames IA 50011   For more information contact: ***drajewsk@iastate.edu***

Introduction

- We evaluate the environmental influence of wind turbines on agricultural crops through detection of reduced wind speed, enhanced turbulence, and perturbations in pressure around wind turbines according to the conceptual model of flow around agricultural shelterbelts described by Wang and Takle (1995) (Fig. 1). Crops surfaces additionally alter surface drag and therefore wind power availability. *Understanding the combined interaction when agricultural crops are raised over vast regions within wind farms is essential to optimize the combination of these two co-located energy sources.*
- The above interactions *may or may not* be significant to impact crop production. Numerical modeling of a hypothetical large wind farm by Baidya Roy et al. (2004) indicated reductions in surface wind, enhanced(decreased) nighttime(daytime) temperature, lower relative humidity, and increased evapo-transpiration. Warmer nighttime temperatures were reported in several turbine lines downstream of the San Gorgoino wind farm (Baidya Roy and Traiteur 2010).
- Satellite observations of offshore wind farms (Christiansen and Hasager, 2005) detect mean wind speed and turbulence in the wake of the wind turbines reaching to the surface.

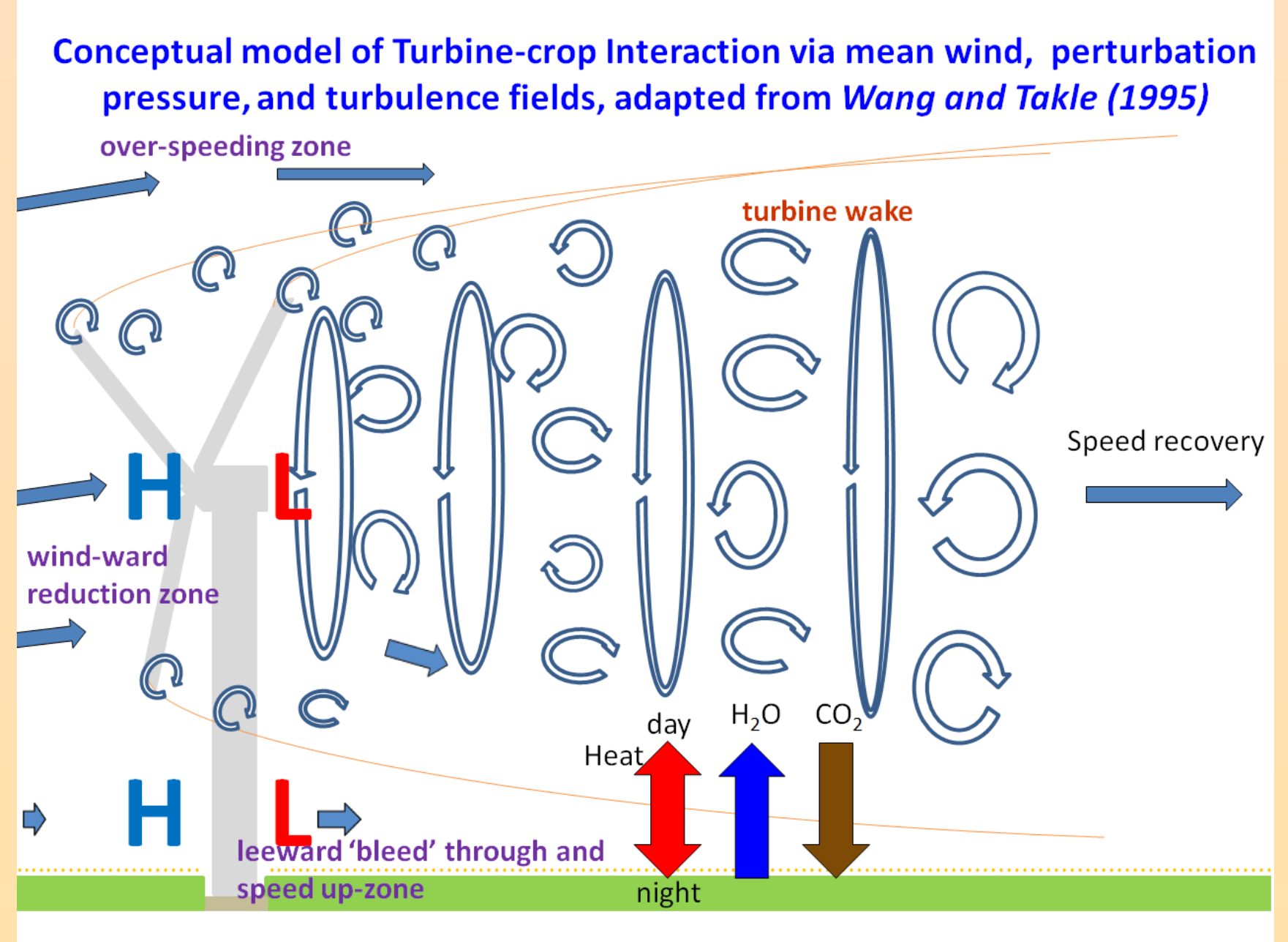

Fig. 1

Crop Wind Energy eXperiment (CWEX)

- Quantifying possible changes on croplands by wind farms is difficult without having sufficient observations at least upwind and downwind of wind turbine towers.
- Flux towers (similar to Fig. 2a) were assembled by the National Laboratory for Agriculture and the Environment (NLAE), the National Center for Atmospheric Research (NCAR) and Iowa State University (ISU) within the southern edge of a large wind farm to measure differences in wind speed, temperature, relative humidity, turbulence, H_2O, and CO_2 during the summer of 2010 and 2011. Wind profiling LiDARs from the University of Colorado and the National Renewable Laboratory (NREL) were placed north and south of the B3 turbine to measure wakes from 40 to 220 m above the surface.
- Fig. 2b identifies the location of the flux towers and wind cube LiDARs in 2011. The stations were positioned ahead of and behind the B2 turbine to get measurements over several rotor diameter distances (D, D=74 m) from the turbine line: upstream (x=-1.5 D), near wake (x=3.5 D), middle wake (x=9 D) and far wake (x= 13 D) as described in Rajewski et al. (2012).

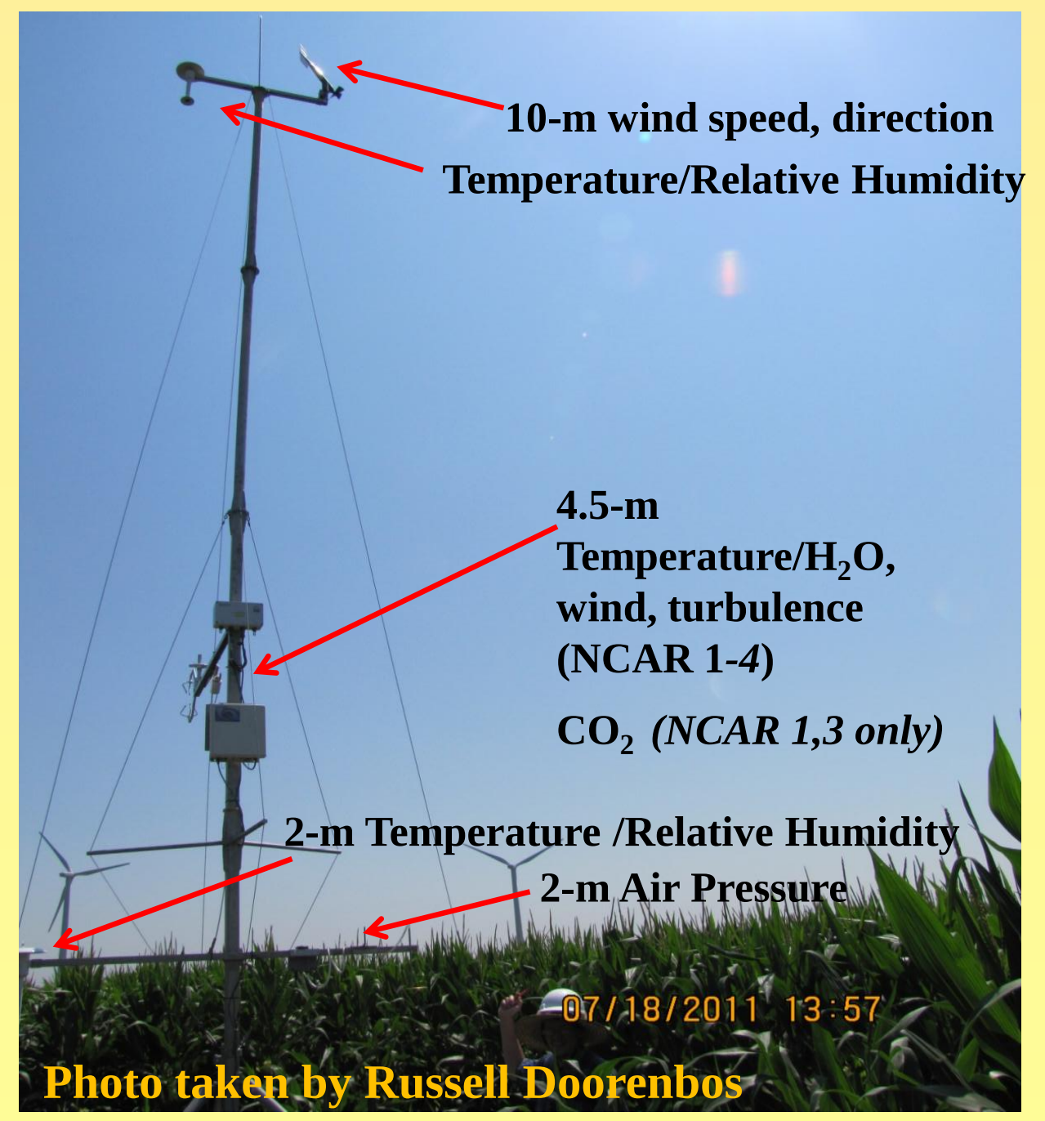

Photo taken by Russell Doorenbos

Fig. 2a

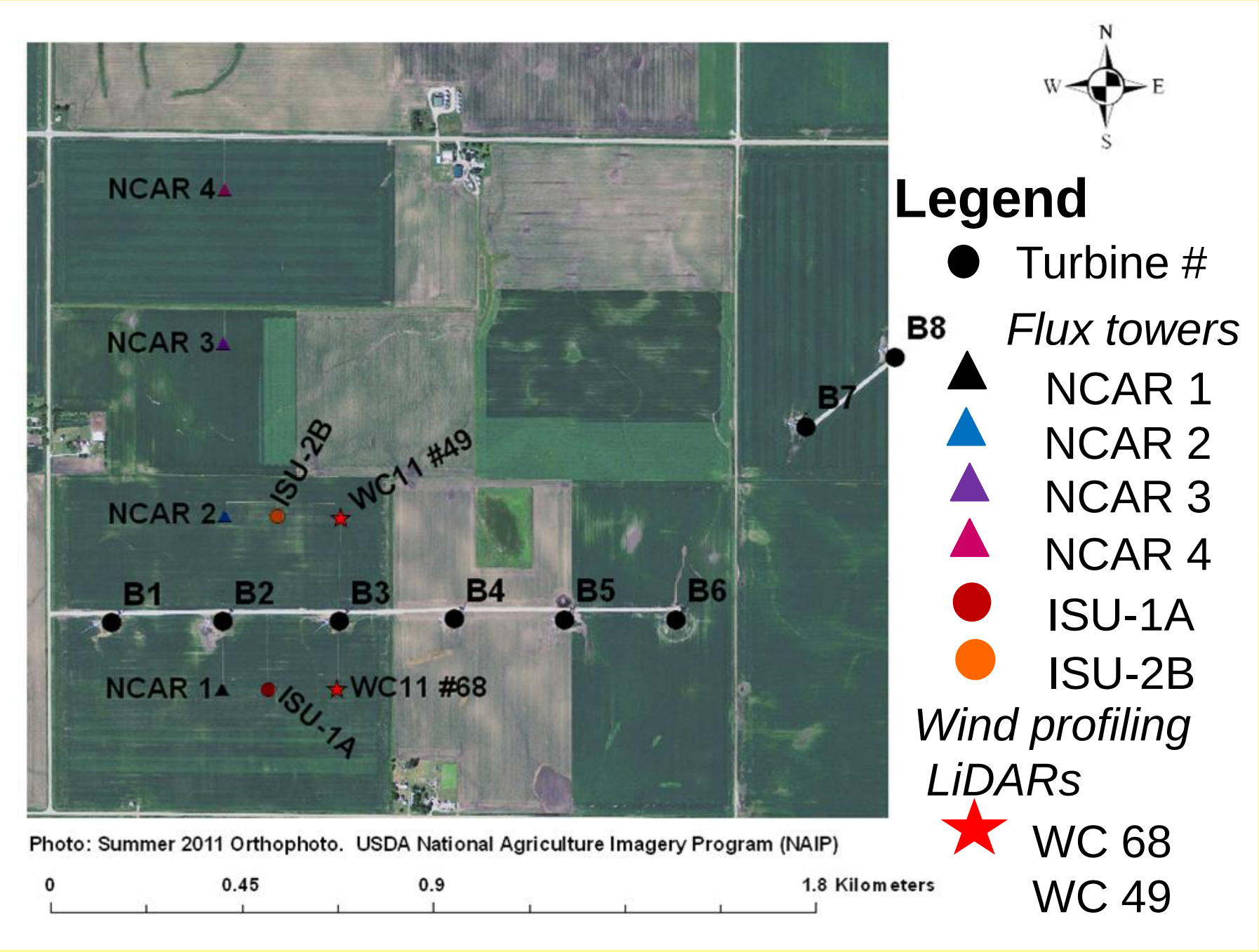

Photo: Summer 2011 Orthophoto. USDA National Agriculture Imagery Program (NAIP)

Fig. 2b

Diurnal differences in crop microclimate

- Flux averages at 15 and 30 minute intervals were computed from the 20 Hz measurements
- Difference fields were calculated between the upstream reference flux tower (NCAR 1) and each downstream wake location (NCAR 2,3,4) for appropriate wake wind direction windows with an expansion factor of 5 degrees from the turbine rotor disk (e.g. Barthelmie et al. 2010) when the turbine wake could be detected at the surface. The south-centerline wake assumes SSE to SSW wind directions whereas the west no-wake is for wind directions slightly WSW to slightly WNW.
- Scatter plots of non-wake westerly flow and wake southerly flow in Fig. 3 and Fig. 4 are represented according to changes in the reference flux tower thermal stability, (z/L). (z/L is positive during the night and negative for the daytime). Observations are filtered to omit rainfall events and other occurrences of sensor malfunction.

West no-wake **South center-line wake**

10-m Wind speed

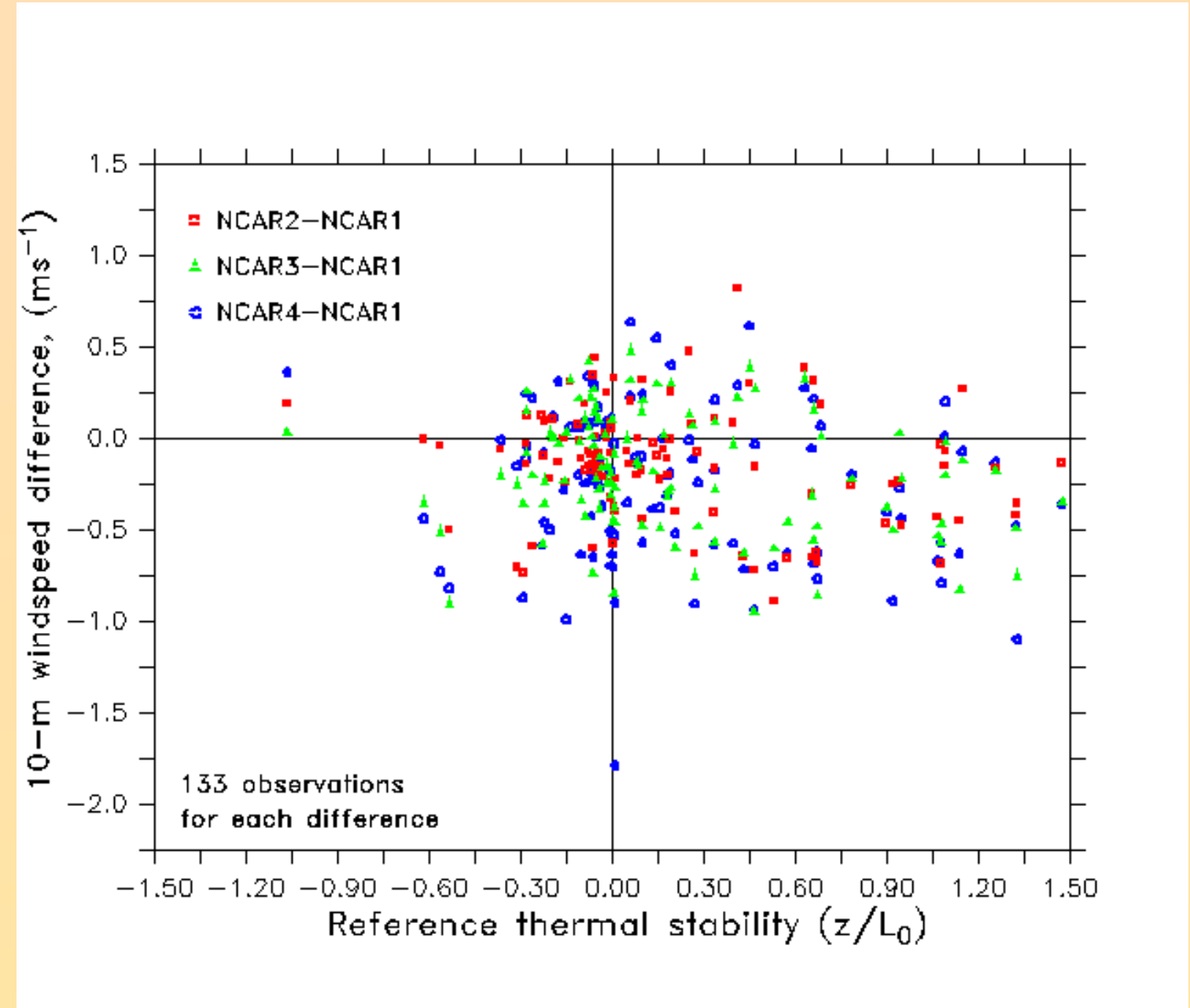

Fig. 3a

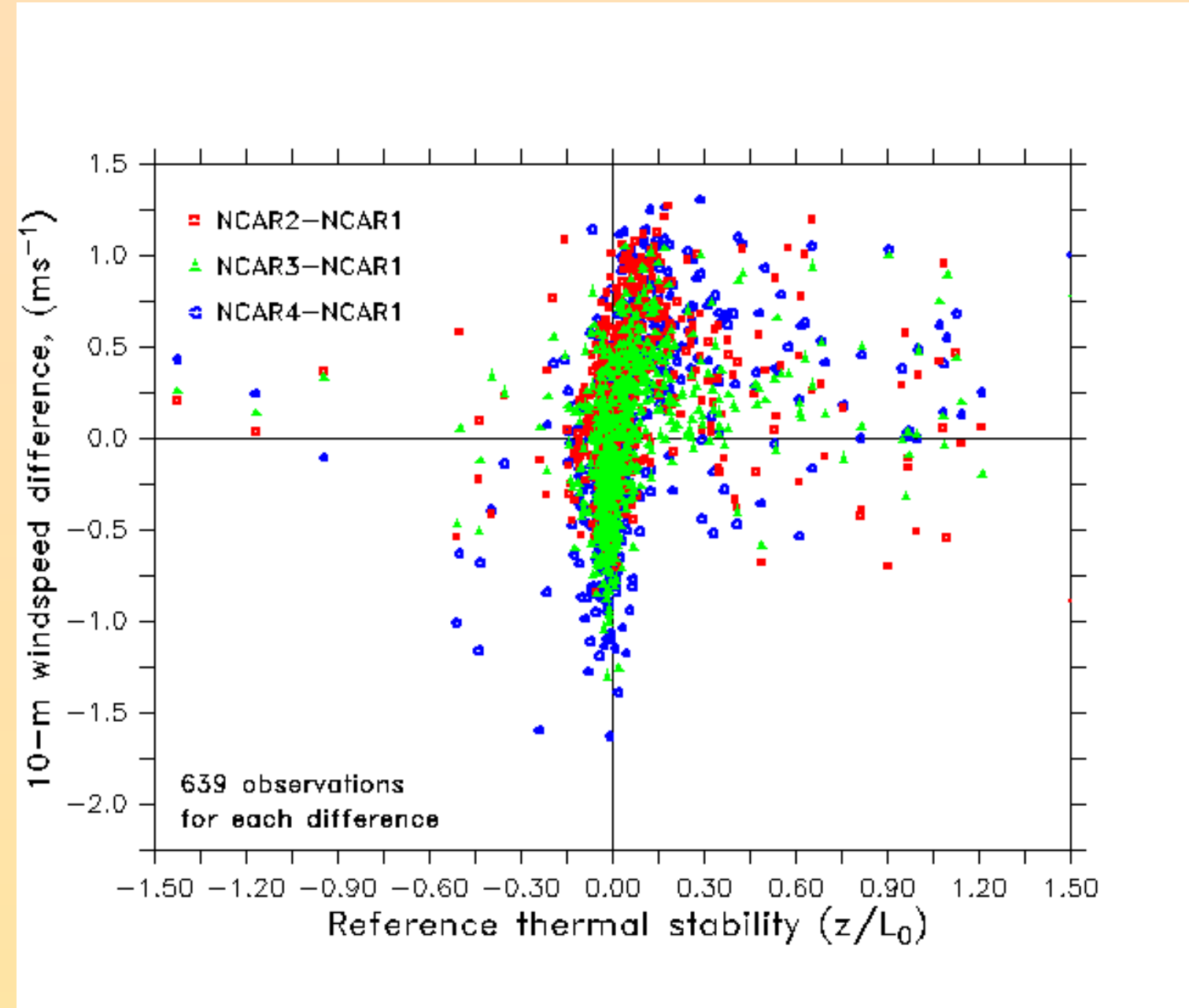

Fig. 3b

- The no-wake case features considerable variation around the zero-line for both daytime and nighttime conditions (Fig. 3a). In the south case, wind speeds are reduced during the daytime especially at the northernmost site (NCAR 4) and all stations north of the turbine line feature a sharp nocturnal over-speeding behind the turbines in Fig. 3b. Nighttime turbulence is also enhanced in the flux stations north of the turbine line.

West no-wake **South center-line wake**

10-m Temperature

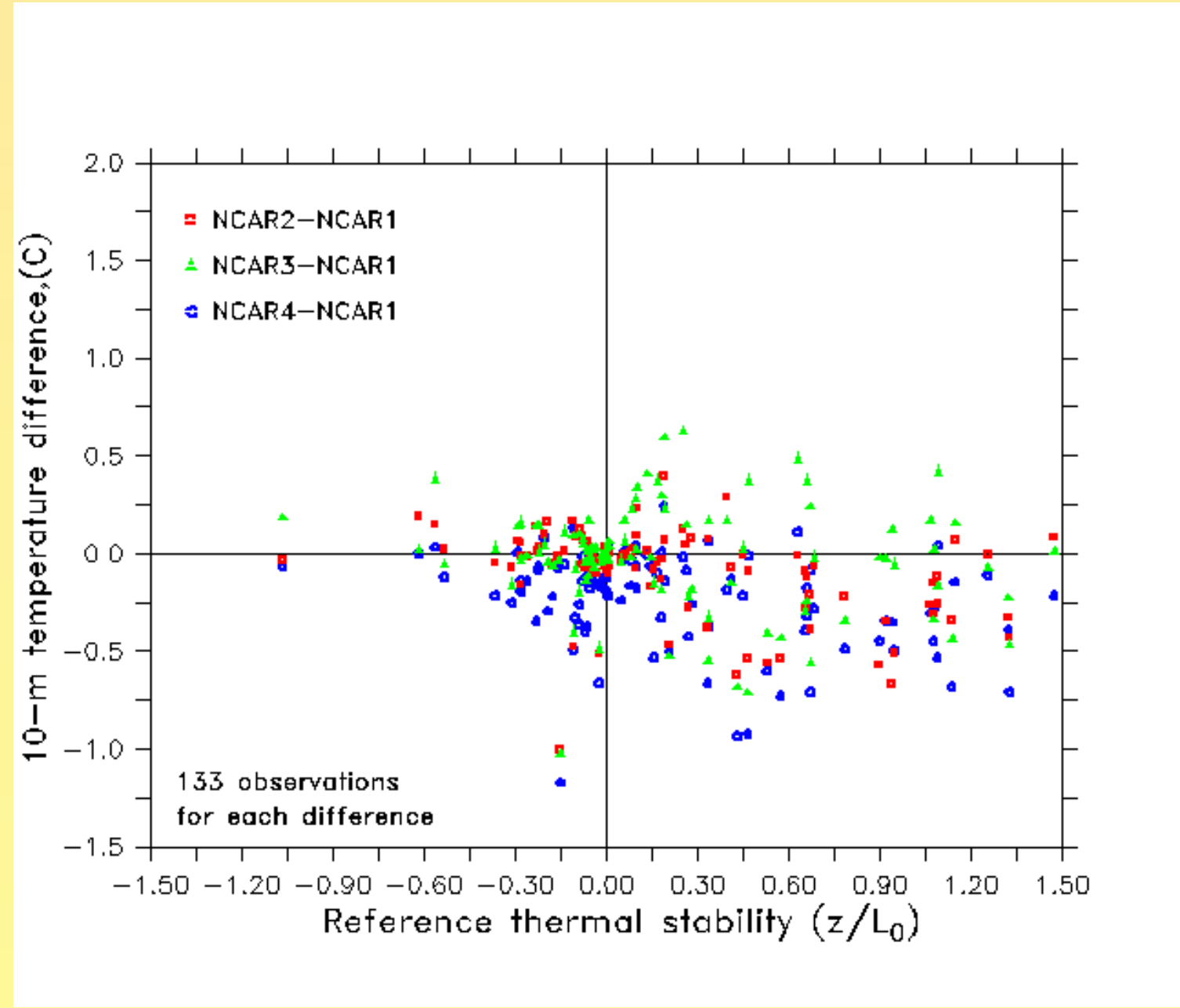

Fig. 4a

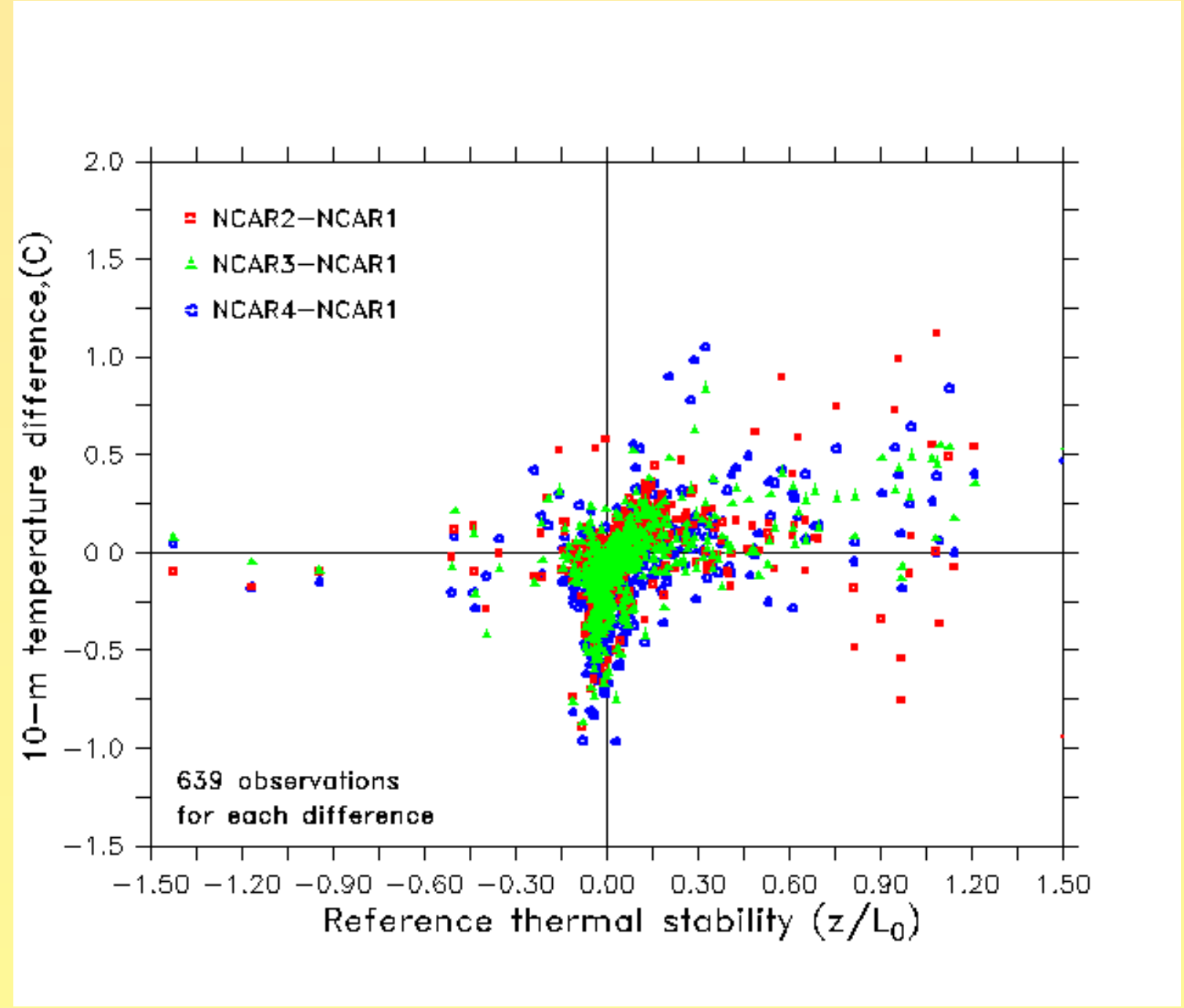

Fig. 4b

- The difference in temperature behaves similar to the wind speed in the west case (Fig. 4a). For southerly flow all sites report cooler above-canopy temperatures by 0.5-1.0 °C for sunny, windy conditions and slightly warmer temperatures for the nightly periods with some wind speed (Fig. 4b). The turbine-modified flow fields enhance downward transport of heat at night but the effect is less noticeable during the daytime when high wind speed and deep mixing dominate the 15-minute averaged motions above the crop canopy.

Daytime 30-minute fluxes of heat, H_2O, and CO_2

West composite **South composite**

Sensible and Latent Heat Flux

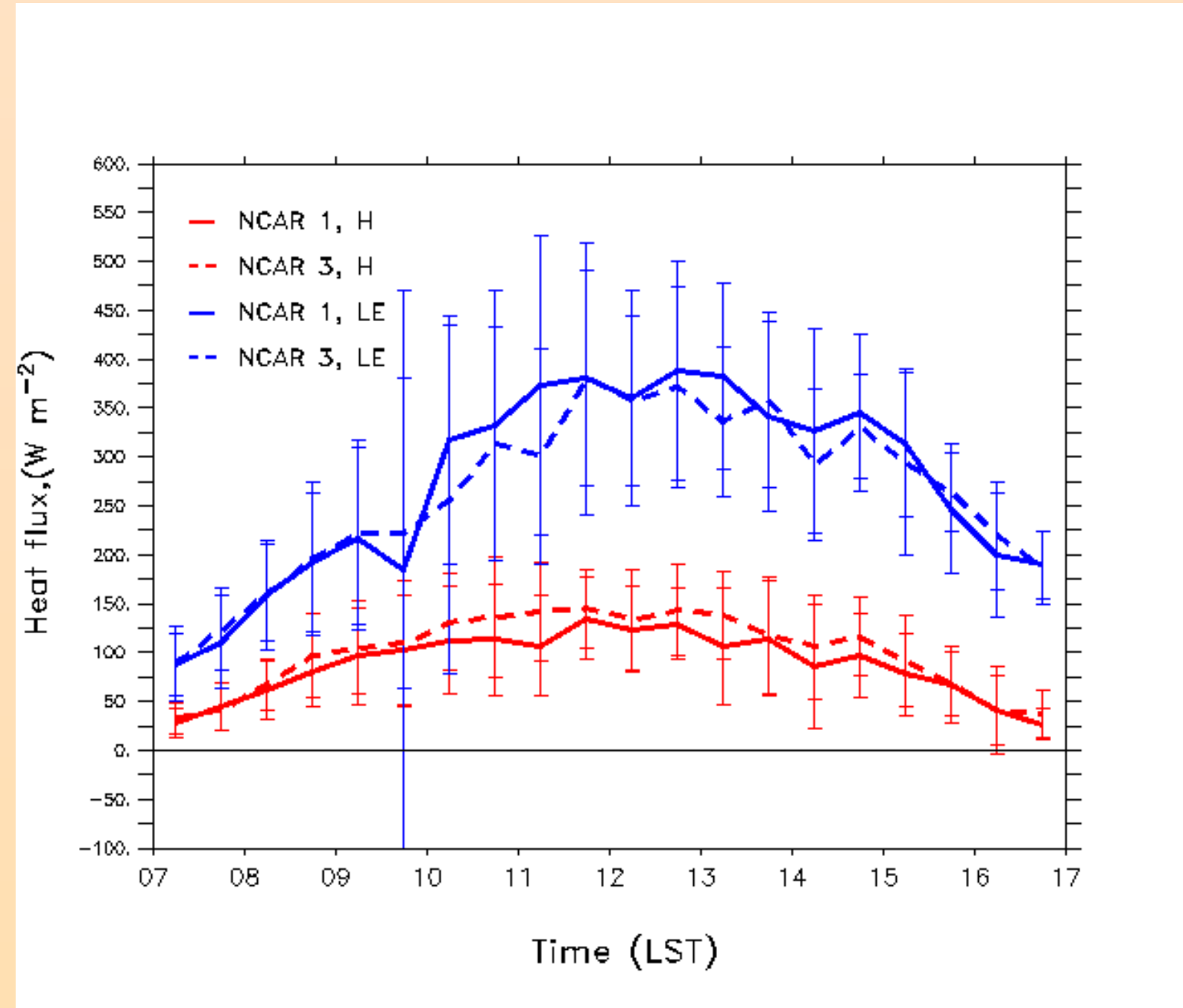

Fig. 5a

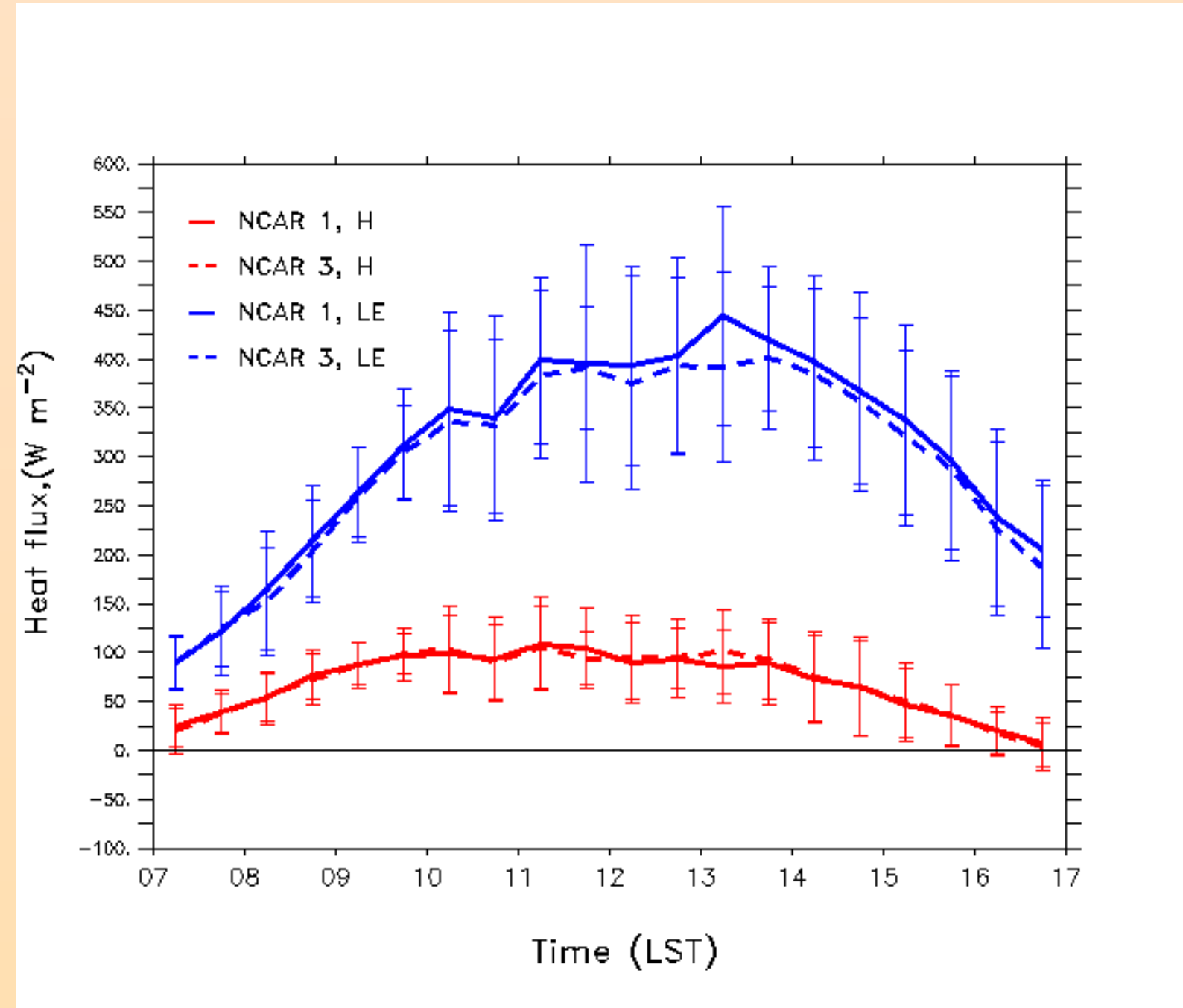

Fig. 5b

Upwind vs. Downwind CO_2 flux

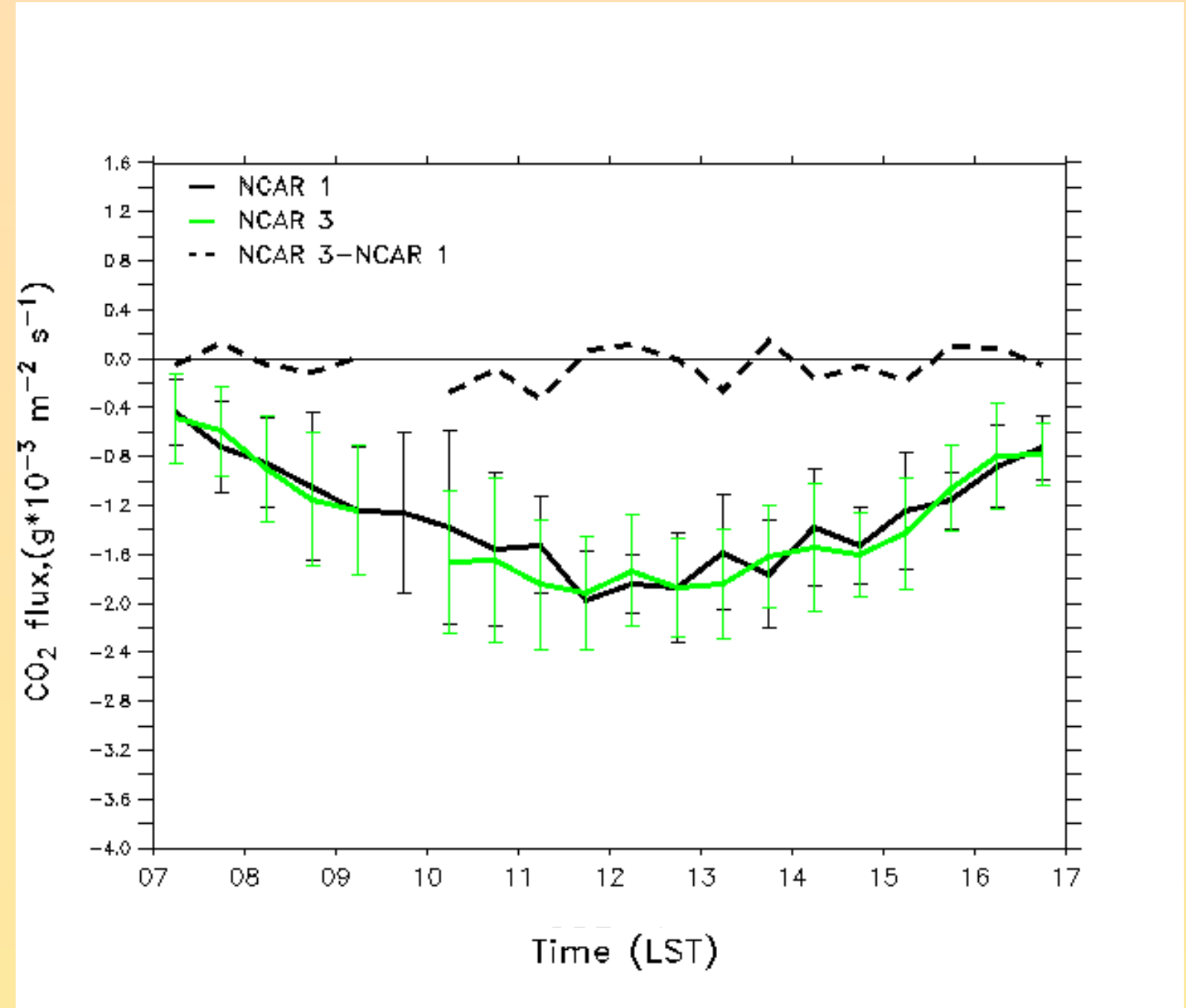

Fig. 6a

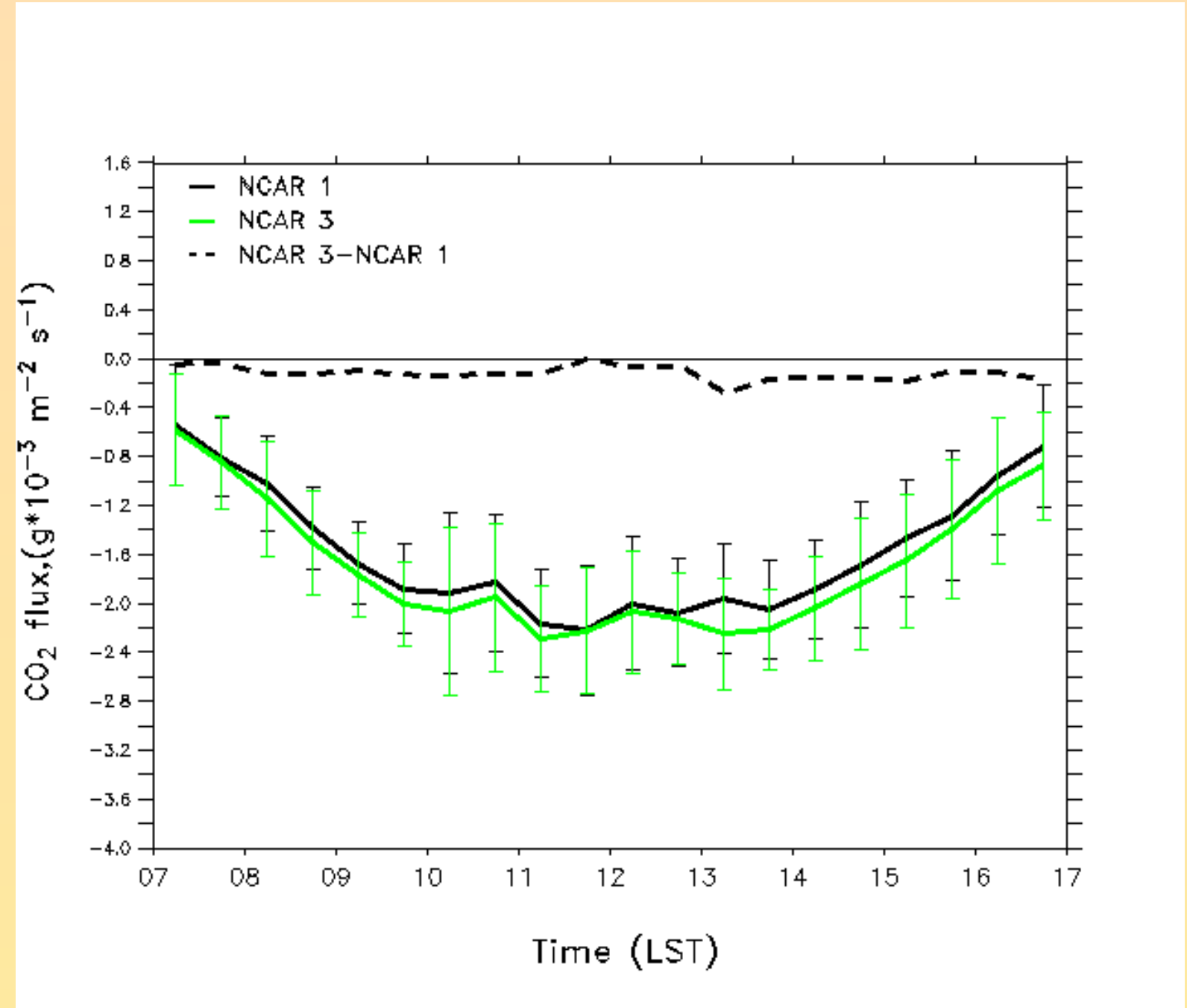

Fig. 6b

- The west and south composites exhibit high variability among the sensible and latent heat flux accordingly since each composite represents multiple days of similar wind directions. The west case, presupposing no turbine influence, in Fig. 5a demonstrates how differences in land management and inter-field variability between the NCAR 1 and 3 can lead to differences in the energy fluxes.
- The south case also shows mediocre differences in flux for Fig. 5b, but the position of the turbine wake is the dominating factor and can only be hinted for these daily averages. Winds from the SSE or SSW favor the position of the turbine wakes to increase the energy fluxes at NCAR 3.
- CO_2 fluxes are also highly variable in both the west and the south composites (Fig. 6a-b) with slightly more carbon exchange north of the turbines for southerly flow. The overall pattern of enhanced canopy CO_2 flux within wind farms is plausible for verification in both short periods (e.g. a few hours) and for an accumulation of the net ecosystem exchange over the growing season.

Acknowledgements

The author recognizes several individuals and organizations in the CWEX studies. John Prueger, Jerry Hatfield, and Dick Pfeiffer from NLAE offered assistance in instrumentation and data processing from 2010 and Steve Oncley, and Tom Horst from NCAR led the instrumentation in the 2011 study. Julie Lundquist from NREL and Michael Rhodes from the University of Colorado provided LiDAR data to facilitate detection of the wind turbine wakes. Graduate and undergraduate students, Russell Doorenbos and Kristopher Spoth, respectively, are recognized for their assistance in experimental design, instrumentation deployment/break down, data management, and post processing techniques. Research adviser, Gene Takle, offered valuable insights in the experiments and analysis. Support was provided by the NCAR Earth Observing Laboratory and the National Science Foundation Grant # EPS-1101284.

IOWA STATE UNIVERSITY
OF SCIENCE AND TECHNOLOGY

IOWA EPSCoR

U.S. DEPARTMENT OF ENERGY

References

Baidya Roy, S.B., S.W. Pacala, and R.L. Walko, 2004: Can large wind farms affect local meteorology?, *J. Geophys. Res.-Atmos.*, **109**, D19101.
Baidya Roy, S.B, and J.J. Traiteur, 2010: Impact of wind farms on surface air temperatures. Proc. Natl. Acad. Sci. http://dx.doi.org/10.1073/pnas.1000493107.
Barthelmie, R. J., and Coauthors, 2010: Quantifying the Impact of wind turbine wakes on power output at offshore wind farms. *J. Atmos. Oceanic Technol.*, **27,** 1302–1317. doi: http://dx.doi.org/10.1175/2010JTECHA1398.1.
Christiansen, M.B., and C.B. Hasager, 2005: Wake effects of large offshore wind farms identified from satellite SAR. *Remote Sens. Environ.*, **98**, 251-268.
Rajewski, D. A. and co-authors, 2012: CWEX: Crop/Wind-energy Experiment: Observations of surface-layer, boundary-layer and mesoscale interactions with a wind farm, *Bull. of the Americ. Meteorol. Soc.* (in review).
Wang, H., and E. S. Takle, 1995: A numerical simulation of boundary-layer flows near shelterbelts. *Bound.-Layer. Meteor.*, **75,** 141-173.